Soft Matter

Dynamic Article Links

Cite this: *Soft Matter*, 2012, **8**, 9177

www.rsc.org/softmatter

PAPER

Complex effects of molecular topology on diffusion in entangled biopolymer blends

Cole D. Chapman,[b] Sachin Shanbhag,[c] Douglas E. Smith[b] and Rae M. Robertson-Anderson*[a]

Received 2nd June 2012, Accepted 20th July 2012
DOI: 10.1039/c2sm26279g

By combining single-molecule tracking with bond-fluctuation model simulations, we show that diffusion is intricately linked to molecular topology in blends of entangled linear and ring biopolymers, namely DNA. Most notably, we find a previously unreported non-monotonic dependence of the self-diffusion coefficient for linear DNA on the fraction of linear DNA comprising the ring-linear blend, which we argue arises from a second-order effect of ring DNA molecules being threaded by varying numbers of linear DNA molecules. Results address several debated issues regarding molecular dynamics in biopolymer blends, which can be used to develop novel tunable biomaterials.

Introduction

Entangled polymers display complex diffusional transport properties that are strongly dependent on molecular concentration, length, and topology. One such system of great interest is DNA, which is not only an important biopolymer, but has also served as a powerful model system for probing general polymer physics questions.[1–4] While most progress has focused on monodisperse linear and branched polymers, blends of polymers of varying lengths and topologies are favored in practical materials engineering to effectively tune properties such as miscibility, strain hardening, *etc.*[5,6] Biological cells, which exhibit remarkable mechanical properties, also contain a mixture of nucleic acid and protein polymers of varying topologies.

The most powerful theoretical concept in entangled polymer dynamics is the tube model, which postulates that each individual entangled polymer is effectively confined, by the surrounding molecules, to diffuse in a tube-like region parallel to its contour (*i.e.* reptation). While originally developed for polymer melts, the tube model has been successfully extended to polymer solutions using "blob" theory,[7–9] in which each chain is divided into correlation blobs and the solution is modeled as a melt of chains with monomer size (*i.e.* Kuhn length) equal to the blob size. While the chain-end mediated process of reptation is the foundation of much of our present understanding of the dynamics of linear and branched polymers, extension of the tube model to ring polymers, which have no ends by which to execute standard reptation, is nontrivial and recognized as a major challenge.[10–27] Further, experimental data on entangled rings is highly conflicting[13–15,23,28] due, in part, to the extreme difficulty of synthesizing samples of purely ring polymers devoid of linear contaminants,[23,29] coupled with the fact that small quantities of linear polymers appear to dramatically alter the rheological properties of ring polymer melts.[12,14,23,30] Nonetheless, blends of linear and ring polymers hold great promise as viscoelastic materials and fluids with highly tunable properties.

Recently, we used single-particle tracking to measure self-diffusion coefficients of linear and ring DNA molecules in solutions of entangled linear or ring DNA, and observed dramatic effects of molecular topology.[18,31] In these studies, tracked linear or ring molecules were added to each solution at essentially infinite dilution, so "tracer" diffusion coefficients in entangled solutions of purely linear or purely ring DNA were measured. Tracer diffusion coefficients exhibited a strong and complex dependence on the topology of both the tracer and the surrounding entangling molecules, and this dependence was most dramatic for the longest molecular lengths and highest solution concentrations examined (*i.e.* highest degree of entanglements). Diffusion in blends containing significant fractions of both ring and linear molecules (ring-linear blends) is expected to exhibit even richer behavior.

In ring-linear (RL) blends, rings can become threaded by their linear counterparts, in which case the only available diffusive mechanism is predicted to be *via* the threading linear polymers releasing their constraints by unthreading themselves (*via* reptation).[10,26,32,33] This constraint release process, for which there is indirect experimental evidence,[18,23,27] is much slower than reptation. Several other ring polymer configurations have also been conjectured in RL blends including once-threaded, unthreaded-linear, and unthreaded-branched.[10,16,26,33] Each configuration relies on different diffusive mechanisms, but the extent to which each configuration and diffusive process play a role in RL blends is still debated.[10,19,26,27]

[a]*Department of Physics, University of San Diego, San Diego, CA 92110, USA. E-mail: randerson@sandiego.edu*
[b]*Department of Physics, University of California San Diego, La Jolla, CA 92093, USA*
[c]*Department of Scientific Computing, Florida State University, Tallahassee, FL 32306, USA*

This journal is © The Royal Society of Chemistry 2012

Rheological studies have examined bulk properties of RL blends such as viscosity, relaxation spectra and terminal relaxation times,[12,14,23,24,30] attempting to test theoretical predictions.[10,19,33] While previous studies have all found a larger than expected rise in viscosity of ring polymer melts upon addition of small amounts of linear polymers, the dependence of viscosity on the fraction of linear polymers in the blend (ϕ_L) remains unclear. Some experimental and simulation studies have reported a non-monotonic dependence of viscosity on ϕ_L with a maximum reached at $\phi_L \approx 0.5$,[34,35] while others have found that viscosity consistently increased with ϕ_L, approaching but never surpassing the value for a pure linear polymer melt.[16,21] Rings have also been shown to have shorter relaxation times and different relaxation spectra than linear polymers of equal length.[4,12,14,23,36] However, the purity of the ring samples and extent to which the rings are entangled in each of these studies remains controversial.

Molecular diffusion in RL blends has been examined in recent experiments[24,27,37–39] and simulations[22,40] which have reported conflicting results with multiple theoretical interpretations. Most recently, NMR was used to measure the dependence of the average blend self-diffusion (D_{blend}) and ring polymer self-diffusion (D_R) on ϕ_L. While D_R decreased linearly with increasing ϕ_L, D_{blend} showed a non-monotonic dependence on ϕ_L with a minimum reached at $\phi_L \approx 70\%$.[24] These results contrast with previous findings reporting that blend composition has little effect on diffusion in RL blends.[11,41]

Previously, we implemented a Monte Carlo simulation approach to model RL blends, using a simple bond-fluctuation model (BFM) with discretized polymers on a lattice. The predictions of the model were consistent with our experimental results described above.[18,31] In addition, we predicted that the self-diffusion coefficient for ring polymers (D_R) would decrease nonlinearly with the fraction of linear polymers in the blend (ϕ_L), decreasing more rapidly at low ϕ_L and slowly reaching a plateau at the highest ϕ_L.[20] We also predicted that the linear polymer self-diffusion coefficient (D_L) would decrease at low ϕ_L and reach what we believed to be a ϕ_L-independent plateau around $\phi_L \approx 30\%$.

In this article, we present experimental and simulation results that, for the first time, systematically characterize the effect of molecular diffusion of both linear and ring molecules on blend composition in entangled ring-linear blends.

Methods

We have chosen to use double-stranded DNA as our model polymer for the described experiments, as DNA, beyond its biological importance, has been well established as a model system for probing fundamental questions in polymer physics.[1,3,4] Further, DNA is amenable to several experimental techniques which are advantageous for the present studies including preparation of ring constructs,[23,29,42] fluorescent-labeling and single-molecule tracking of tracer molecules. While DNA is less flexible than typical synthetic polymers, a well-accepted notion in current polymer theory is that polymers of varying chemical composition, length and flexibility, when scaled according to the number of monomers or "blobs", exhibit universal properties.[7,9]

Details of all experimental techniques used, briefly summarized below, have been thoroughly described in ref. 18, 31, 42 and 43. Double-stranded DNA molecules, with contour lengths of 11 and 45 kilobasepairs (kbp), corresponding to 3.74 μm (~75 persistence lengths) and 15.3 μm (~305 persistence lengths), respectively, were prepared by replication of cloned plasmid and fosmid constructs in *E. coli*, followed by extraction and purification. Restriction enzymes (BamHI, ApaI) and Topoisomerase I were used to prepare linear and ring forms, respectively. Blended solutions of varying weight fractions of linear and ring DNA, in aqueous buffer (10 mM Tris–HCl (pH 8), 1 mM EDTA, 10 mM NaCl), with overall solution concentrations (c) of 0.1, 0.5 and 1.0 mg ml^{-1} were prepared, as depicted in Fig. 1. A trace amount ($<10^{-3}c$) of linear or ring DNA (tracers), labeled with YOYO-I (Invitrogen) for tracking, was mixed with the desired blended DNA solution (see Fig. 1), and imaged with a fluorescence microscope using a 60× 1.2 NA water-immersion objective. Note that because the tracer concentration is <1/1000 of the overall solution concentration, the presence of the tracers can be neglected when determining the overall solution concentration c and the weight fraction of linear DNA in the blended solution (ϕ_L). As reviewed in ref. 3, YOYO-I labeling slightly increases both the persistence length and contour length of DNA by ~1.34. However, the number of persistence lengths and basepairs per persistence length remain unchanged. This small length change is expected to have a minimal effect on the dynamics of the tracer DNA,[31,42] such that tracers are representative of the unlabeled DNA of equal length and topology in the solution. Images were captured at 10 frames per sec with a high-resolution CMOS camera (Hamamatsu). Center-of-mass (x, y) coordinates of >200 paths of different molecules were tracked, and the

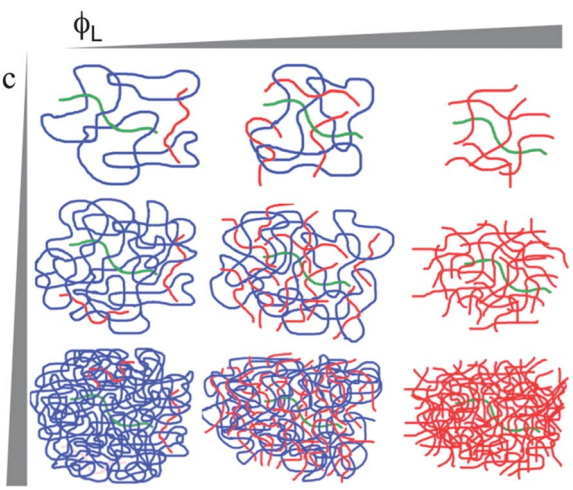

Fig. 1 Schematic of experimental parameter space probed for ring-linear DNA blends. To track the center-of-mass motion of single linear molecules (to determine D_L) in ring-linear blends, a trace amount of fluorescent-labeled (green) linear tracer chains are embedded in entangled solutions of ring (blue) and linear (red) DNA of varying solution concentration (c) and linear chain fraction (ϕ_L). Concentration increases from 0.1 mg ml^{-1} (top row) to 1.0 mg ml^{-1} (bottom row) and linear fraction increases from 0 (left column) to 1 (right column). Identical experiments are carried out using fluorescent-labeled ring tracers to determine D_R.

This journal is © The Royal Society of Chemistry 2012

Einstein relation $\langle x^2 \rangle = \langle y^2 \rangle = 2Dt$ was used to determine diffusion coefficients. Errors were estimated using the bootstrap method.[44]

We used the lattice bond-fluctuation model to simulate ring-linear blends and predict molecular self-diffusivities. The underlying protocol, which has been described and validated in sufficient detail previously,[20,22,40] involves placing and moving beads corresponding to monomers of linear and ring polymers on a simple cubic lattice, subject to the constraints of excluded volume, bond non-crossability, and chain connectivity. The self-diffusion coefficient is computed from the mean-squared displacement of the center-of-mass of the polymers. In the BFM, the number of beads per polymer N at a total fractional lattice occupancy of $f = 0.5$ is related to the number of Kuhn lengths per polymer N_K *via* $N = 0.83N_K$.[45] Using blob theory, the effective Kuhn length for concentrated solutions (*i.e.* the correlation blob size) is calculated *via* $R_g(c/c^*)^{-0.78}$, where R_g is the radius of gyration and c^* is the overlap concentration.[4] Thus for the 45 kbp DNA at $c = 1$ mg ml^{-1} the blob size is ~58 nm (N_K = 263),[42,43] and as such is equivalent to $N = 316$ beads per polymer at a total fractional lattice occupancy of $f = 0.5$ in the BFM.[20,31] We also performed simulations at $f = 0.25$ (corresponding to c = 0.5 mg ml^{-1}) and $f = 0.05$ ($c = 0.1$ mg ml^{-1}). For each f, we spanned $0 \leq \phi_L \leq 1$, adjusting the simulation box size and number of replicas to ensure >500 molecules were used to estimate the self-diffusivity.

Results

Measured diffusion coefficients for linear and ring tracer DNA molecules are plotted as a function of linear fraction ϕ_L in Fig. 2. Molecular lengths and solution concentrations range from well-above to well-below the critical concentration for entanglement (c_e), above which linear molecules exhibit reptation dynamics (c_e ~ 0.4 mg ml^{-1}, ~1.3 mg ml^{-1} for 45 kbp, 11 kbp DNA, respectively[31]).

For the 45 kbp DNA at $c = 1.0$ mg ml^{-1} (Fig. 2a) both D_L and D_R are highest in a pure solution of rings ($\phi_L = 0$). D_R decreases rapidly as ϕ_L increases, dropping by a factor of ~4 with only 20% linear molecules, and by a factor of 8 at 40% linear DNA. For 0.4 < ϕ_L < 1, D_R continues to monotonically drop, albeit with a weaker ϕ_L dependence, reaching a minimum, ~17 times slower than $D_R(\phi_L = 0)$, at $\phi_L = 1$.

Interestingly, our results for D_L display a non-monotonic dependence on the linear fraction ϕ_L, steadily decreasing by a factor of ~3 as ϕ_L increases from 0 to 50%. As ϕ_L is further increased D_L steadily increases, almost doubling as ϕ_L increases to 1. To our knowledge, such behavior was not anticipated by any prior experimental or theoretical work.

At $c = 0.5$ mg ml^{-1} (Fig. 2b), trends similar to the 1.0 mg ml^{-1} case are found for both D_L and D_R, although the dependence on ϕ_L is weakened. D_R decreases by a factor of ~3 as ϕ_L increases from 0 to 1, with a ~2× reduction at $\phi_L = 0.2$. Likewise, D_L displays a modest non-monotonic dependence on ϕ_L, reaching a minimum at $\phi_L = 0.6$.

For the lowest concentration (0.1 mg ml^{-1}, Fig. 2c), which is well below the critical concentration for entanglement, both D_L and D_R showed little dependence on blend composition, demonstrating that the complex dependence of molecular diffusion on blend composition is due to molecular entanglements. Similar results were found for ~4× shorter (11 kbp) DNA at 1.0 mg ml^{-1} (Fig. 2c); however the 11 kbp DNA does exhibit a modest decrease in D_R with ϕ_L similar to that of the entangled blends discussed above but much weaker. As the 11 kbp, 1.0 mg ml^{-1} system is quite close to the critical concentration for entanglement (c_e ~1.3 mg ml^{-1}), this small decrease is expected as entanglements begin to form, and further demonstrates the dependence of the results on molecular entanglements.

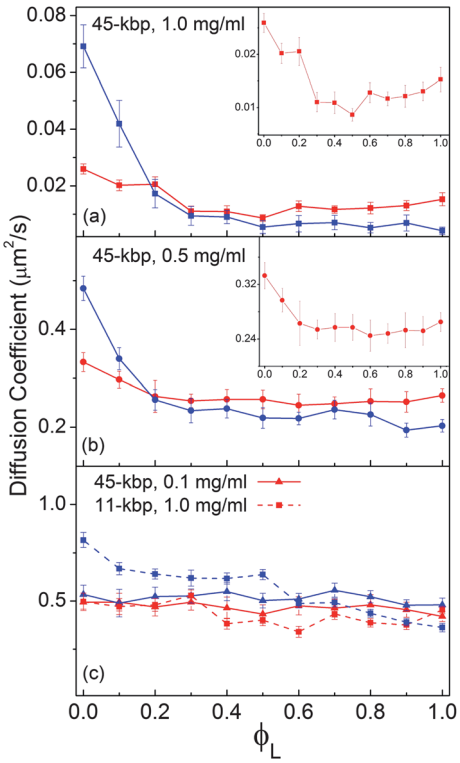

Fig. 2 Measured self-diffusion coefficients *vs.* fraction of linear DNA (ϕ_L) in ring-linear blends. Self-diffusion coefficients for ring (blue) and linear (red) DNA in ring-linear blends at three overall solution concentrations, 0.1 mg ml^{-1} (triangles), 0.5 mg ml^{-1} (circles), and 1.0 mg ml^{-1} (squares), and two molecular lengths, 45 kbp (solid lines) and 11 kbp (dashed lines) are shown. The molecular lengths and solution concentrations displayed in each panel, (a), (b), and (c), are listed in the top left corner of the corresponding panel. Insets show zoomed in plots for linear DNA with appropriately adjusted y-axes.

If our BFM simulations capture the essential physics, the mapping between experimental diffusivities (μm^2 s^{-1}) and BFM diffusivities ((lattice units)^2/(Monte Carlo Step)) is expected to be proportional. Fig. 3 presents simulation and experiment results on the same plot, normalized such that $D_L^* = D_L(\phi_L = 1, c = 1$ mg ml^{-1}) = $D_L(\phi_L = 1, f = 0.5)$.

At the highest ($f = 0.5$) and lowest ($f = 0.05$) concentrations, simulations match experimentally observed trends quite well over the entire ϕ_L range. For the 0.5 mg ml^{-1} ($f = 0.25$) case, experimental and simulation results show similar variations of D_L and D_R with ϕ_L, however the magnitudes of the normalized diffusion coefficients differ by a factor of ~2. We believe this discrepancy arises from the fact that this concentration is in the crossover regime between entangled and dilute polymer dynamics, where peculiarities of the BFM lattice are most

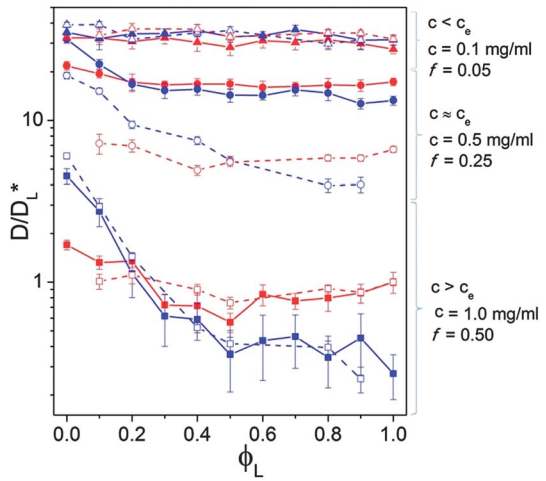

Fig. 3 Comparison between experiment and simulation results for self-diffusion coefficients *vs.* linear fraction ϕ_L in ring-linear blends. Experiment (solid lines) and simulation (dashed lines) results are normalized by $D_L^* = D_L(\phi_L = 1, c = 1 \text{ mg ml}^{-1}) = D_L(\phi_L = 1, f = 0.5)$. Symbols and colors are as in Fig. 2.

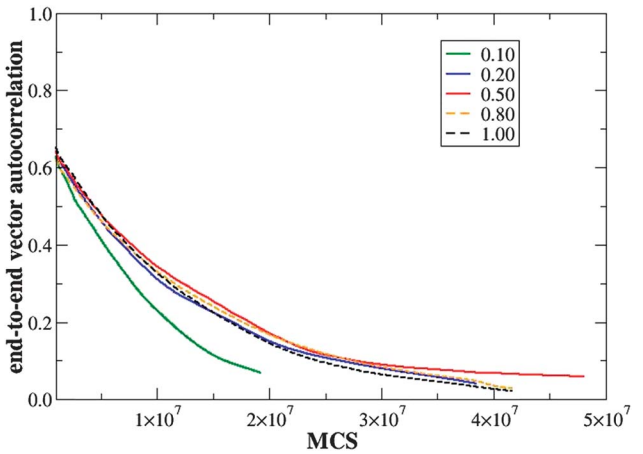

Fig. 4 The decorrelation of the end-to-end vector of the linear chains at $f = 0.5$ for different ϕ_L values (specified in the legend). The relaxation of the end-to-end vector initially slows down as ϕ_L increases from 0.10 to 0.50, and then accelerates as ϕ_L increases from 0.50 to 1.00. These non-monotonic ϕ_L-dependent dynamics are also evident in Fig. 3 and 5.

apparent. For example, previous studies on ring polymers indicate that while both the experiments and the BFM exhibit a crossover from Rouse scaling ($D_R \sim c^{-0.5}$) to reptation scaling ($D_R \sim c^{-1.75}$), and agree in both the dilute (Rouse) and entangled (reptation) regimes, there are noticeable differences in the location ($c_e \sim 0.4$ mg ml^{-1} *vs.* $f_e \sim 0.25$) and sharpness of the transition.[22,31] Future work will examine this discrepancy in more detail, however it is outside the scope of the current study which is focused on entangled ring-linear blends well above c_e.

Importantly, the simulations also exhibit the experimentally observed non-monotonic variation of $D_L(\phi_L)$ at $f = 0.25$ and $f = 0.5$. Because this feature is less prominent than the rapid initial decrease of $D_R(\phi_L)$, we previously noted that $D_L(\phi_L)$ appeared to plateau at $\phi_L \sim 0.3$ in our initial BFM studies.[20] However, the observed minimum in D_L is significant as it is above the measured error in both simulations and experiment. The non-monotonicity is also evident in the autocorrelation of the end-to-end vector in the simulations, which is defined as,

$$p_L(t) = \frac{\langle R_{ee}(t) R_{ee}(0) \rangle}{\langle R_{ee}^2(0) \rangle}$$

where $R_{ee}(t)$ is the end-to-end vector of a linear molecule at time t, and the angular brackets represent an ensemble average over all the linear chains in the system. We used the correlator algorithm, widely used in photon-correlation spectroscopy,[46,47] which allows us to compute $p_L(t)$ on the fly. Fig. 4 shows that as ϕ_L increases, $p_L(t)$ initially decays more slowly. However, beyond a certain ϕ_L, the trend reverses, and $p_L(t)$ decays more quickly as ϕ_L increases.

Discussion

While the slowing of ring polymers at small ϕ_L, due to threading, has received much attention, the non-monotonic variation of $D_L(\phi_L)$ has completely escaped notice. To gain further insight on this feature, we extend the minimal constraint model previously used to explain the variation of $D_R(\phi_L)$.[20]

In the original model, we considered $D_R(\phi_L)$ as a competition between constraint release and pure diffusion, with the slower process controlling the overall rate. Characteristic diffusional decorrelation timescales can be defined *via* $D_i(\phi_L) = R_{g,i}^2(\phi_L)/\tau_i(\phi_L)$, where R_g is the radius of gyration, and i = R (ring) or L (linear). If we ignore the small variation of R_g with ϕ_L (as justified by ref. 19, 35 and 40), and treat the polymers as Gaussian coils, the original minimal constraint model can be rephrased as $\tau_R(\phi_L) = \tau_R(\phi_L = 0) + \tau_{CR}(\phi_L)$, where the constraint release timescale τ_{CR} depends on the number and mobility of the threading linear chains. From primitive path analysis of simulation data, which shrinks polymer contours without violating topological constraints, we find that the average number of linear polymers threading a ring is approximately $\phi_L Z$,[19,20] with Z being the average number of entanglements per molecule in a purely linear polymer melt. Hence, it is reasonable to approximate the Rouse-like contribution as $\tau_{CR}(\phi_L) \sim \tau_L(\phi_L)\, \phi_L Z^2$, which leads to:

$$\tau_R(\phi_L) = \tau_{R0} + c_1 \phi_L Z^2 \tau_L(\phi_L), \quad (1)$$

where c_1 is a constant, and $\tau_{i0} = \tau_i(\phi_L = 0)$, and $\tau_{i1} = \tau_i(\phi_L = 1)$ for i = R or L. This simplified relation has previously been validated by experimental and simulation data.[20]

To extend this model to explain the variation of $D_L(\phi_L)$, we consider a simple empirical form for $\tau_L(\phi_L)$, motivated by experimental findings on binary blends of linear polymers.[48,49] When extremely long linear chains with $Z \gg 1$ are blended (at fraction ϕ_L) with much shorter linear chains, the viscosity or longest relaxation time of the long molecules $\tau_L(\phi_L)$ roughly varies as:

$$\tau_L(\phi_L) \approx \phi_L^2 \tau_{L1} + (1 - \phi_L^2)\tau_0 Z^2$$

where the time-constant τ_0 establishes the constraint-release Rouse relaxation. By analogy, we hypothesize the following simple form for ring-linear blends:

This journal is © The Royal Society of Chemistry 2012

$$\tau_L(\phi_L) = \phi_L{}^2\tau_{L1} + (1 - \phi_L{}^2)[c_2\tau_R(\phi_L)Z^2], \quad (2)$$

where the bracketed term crudely captures the threading of rings *via* a constraint-release Rouse mechanism, and c_2 is an adjustable parameter. While this is a coarse simplification of complex molecular dynamics, the idea here is simply to explore whether a qualitatively plausible form can rationalize the observed trend.

Eqn (1) and (2) are coupled in $\tau_L(\phi_L)$ and $\tau_R(\phi_L)$, with two undetermined dimensionless constants c_1 and c_2, which can be determined by considering eqn (1) in the limit of $\phi_L = 1$, and eqn (2) in the limit of $\phi_L = 0$, respectively. Thus, $c_1Z^2 = (\tau_{R1} - \tau_{R0})/(\tau_{L1})$, and $c_2Z^2 = \tau_{L0}/\tau_{R0}$.

From the diffusivity data at $\phi_L = 0$ and $\phi_L = 1$, at 0.5 mg ml^{-1} and 1.0 mg ml^{-1}, we find $c_1 \sim c_2 \sim 0.01$. In particular, for the 45 kbp, 1 mg ml^{-1} case with $c_1 = 0.008$, and $c_2 = 0.012$, in eqn (1) and (2), we get Fig. 5, which qualitatively captures the non-monotonic variation in $\tau_L(\phi_L)$.

Numerical experimentation with the minimal constraint model indicates that the shape of the curves and the location of the maxima are sensitive to the values of c_1 and c_2. It also points to a necessary criterion for observing the non-monotonic behavior in $\tau_L(\phi_L)$ clearly, *viz.* $\tau_{R0}/\tau_{L0} < 1$ and $\tau_{R1}/\tau_{L1} > 1$, requiring that $D_L(\phi_L)$ and $D_R(\phi_L)$ crossover, as indeed seen in Fig. 2. This criterion is satisfied at large N or high concentrations, where the minimum in D_L is observed most clearly. The model also suggests that as $\tau_{R1}/\tau_{L1} \gg 1$ (perhaps at concentrations and lengths much higher than those explored here), it might be possible to observe minima in D_R as well.

To try to understand the complex interplay of structure and dynamics from a more intuitive standpoint,[50] we first ask, "why does τ_R increase monotonically with ϕ_L?" At low ϕ_L, a small fraction of rings are threaded by linear polymers, and rendered sharply less mobile, while the bulk of rings are unthreaded and diffuse essentially freely. As ϕ_L increases, both the fraction of threaded rings and the number of times a particular ring polymer is threaded increases,[19] causing $\tau_R(\phi_L)$, which is an average over all rings, to increase with ϕ_L. Beyond a certain ϕ_L, which depends on Z and f, all rings are at least "once"-threaded. The slowdown in mobility is substantial when an unthreaded ring is threaded once; it is less so when a once-threaded ring is threaded twice, which qualitatively explains why the rate of increase in $\tau_R(\phi_L)$ tapers off in Fig. 5.

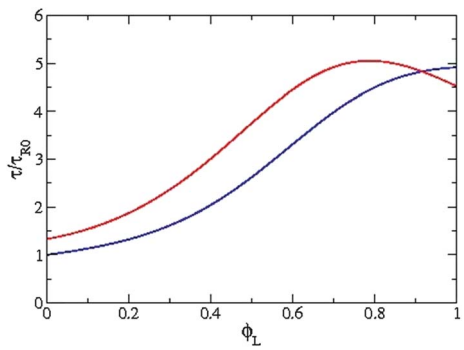

Fig. 5 The solution of eqn (1) and (2) (see text) for $\tau_L(\phi_L)$ (red) and $\tau_R(\phi_L)$ (blue), for the 45 kbp, 1 mg ml^{-1} case with $c_1 = 0.008$, and $c_2 = 0.012$, exhibits non-monotonic variation in $\tau_L(\phi_L)$.

The non-monotonic variation in $\tau_L(\phi_L)$ is more interesting. Previous simulations using primitive path analysis, which indicates how the environment of constraints around a "test" linear polymer varies with ϕ_L,[19] demonstrate that the total number of constraints on a linear test chain remains constant (ring constraints decrease while linear constraints increase with ϕ_L). We can combine this structural information with (i) the monotonic increase in $\tau_R(\phi_L)$ and (ii) $\tau_{R1} > \tau_{L1}$ to explain the non-monotonicity in $\tau_L(\phi_L)$.

At $\phi_L = 1$, the linear test chain is only constrained by surrounding linear chains, all having a timescale τ_{L1}. As ϕ_L decreases, at first, one of these constraining linear chains is replaced by a ring polymer. In this regime ($\phi_L \sim 1$), $\tau_R(\phi_L) > \tau_{L1}$ (Fig. 5), since the average ring is threaded multiple times. From the standpoint of the test chain, it exchanged a more mobile constraint with a less mobile one, causing $\tau_L(\phi_L)$ to initially increase as ϕ_L decreases from 1. Concurrently, however, $\tau_R(\phi_L)$ decreases with decreasing ϕ_L, as discussed above. The net effect is that as ϕ_L decreases further, a larger fraction of the linear constraints are replaced by rings (effect of structure) that are themselves increasingly mobile (effect of dynamics). Thus, $\tau_R(\phi_L)$ and $\tau_L(\phi_L)$ approach each other, and at a certain point $\tau_R(\phi_L) = \tau_L(\phi_L)$. Beyond this point, we begin exchanging less mobile linear constraints with more mobile ring constraints. This is manifested as a maximum in $\tau_L(\phi_L)$ or a minimum in $D_L(\phi_L)$.

Conclusion

In summary, we have combined single-molecule experiments with simulation studies to systematically quantify the dependence of molecular diffusion on molecular topology and intermolecular entanglements in blends of linear and ring biopolymers. Among our findings, we observed a previously unreported and unpredicted non-monotonic dependence of linear polymer diffusion on the fraction of linear polymers in the blend, which we have shown can be explained as a second order effect of the slowed diffusion of threaded rings in the blend. Reported results, which resolve several debated issues in polymer physics and chemistry, may also be used to tune novel biopolymer materials and fluids to exhibit specific viscoelastic properties.

Acknowledgements

We thank M. Harlander-Locke, K. Forey and S. Wright for assistance and Research Corporation and AFOSR for support. SS acknowledges support from the National Science Foundation under Grant no. NSF-CAREER DMR-0953002.

References

1 R. Pecora, *Science*, 1991, **251**, 893–898.
2 C. M. Schroeder, H. P. Babcock, E. S. Shaqfeh and S. Chu, *Science*, 2003, **301**, 1515–1519.
3 E. S. G. Shaqfeh, *J. Non-Newtonian Fluid Mech.*, 2005, **130**, 1–28.
4 R. M. Robertson and D. E. Smith, *Phys. Rev. Lett.*, 2007, **99**, 126001.
5 S. Singla and H. W. Beckham, *Macromolecules*, 2008, **41**, 9784–9792.
6 J. M. Dealy and R. G. Larson, *Structure and Rheology of Molten Polymers: From Structure to Flow Behavior and Back Again*, Hanser Gardner Publications, Cincinnati, 2006.
7 P. G. de Gennes, *Scaling Concepts in Polymer Physics*, Cornell University Press, Ithaca, NY, 1979.

8 R. H. Colby and M. Rubinstein, *Macromolecules*, 1990, **23**, 2753–2757.
9 Y. Heo and R. G. Larson, *J. Rheol.*, 2005, **49**, 1117–1128.
10 J. Klein, *Macromolecules*, 1986, **19**, 105–118.
11 D. Kawaguchi, K. Masuoka, A. Takano, K. Tanaka, T. Nagamura, N. Torikai, R. M. Dalgliesh, S. Langridge and Y. Matsushita, *Macromolecules*, 2006, **39**, 5180–5182.
12 J. Roovers, *Macromolecules*, 1988, **21**, 1517–1521.
13 S. P. Obukhov, M. Rubinstein and T. Duke, *Phys. Rev. Lett.*, 1994, **73**, 1263–1266.
14 G. B. McKenna, B. J. Hostetter, N. Hadjichristidis, L. J. Fetters and D. J. Plazek, *Macromolecules*, 1989, **22**, 1834–1852.
15 J. A. Semlyen, *Cyclic Polymers*, Klwer Academic Publishers, Amsterdam, 2nd edn, 2000.
16 B. V. S. Iyer, A. K. Lele and V. A. Juvekar, *Phys. Rev. E: Stat., Nonlinear, Soft Matter Phys.*, 2006, **74**, 021805.
17 R. M. Robertson and D. E. Smith, *Macromolecules*, 2007, **40**, 8737–8741.
18 R. M. Robertson and D. E. Smith, *Proc. Natl. Acad. Sci. U. S. A.*, 2007, **104**, 4824–4827.
19 G. Subramanian and S. Shanbhag, *Phys. Rev. E: Stat., Nonlinear, Soft Matter Phys.*, 2008, **77**, 011801.
20 G. Subramanian and S. Shanbhag, *Macromolecules*, 2008, **41**, 7239–7242.
21 T. McLeish, *Nat. Mater.*, 2008, **7**, 933–935.
22 B. V. S. Iyer, S. Shanbhag, V. A. Juvekar and A. K. Lele, *J. Polym. Sci., Part B: Polym. Phys.*, 2008, **46**, 2370–2379.
23 M. Kapnistos, M. Lang, D. Vlassopoulos, W. Pyckhout-Hintzen, D. Richter, D. Cho, T. Chang and M. Rubinstein, *Nat. Mater.*, 2008, **7**, 997–1002.
24 S. Nam, J. Leisen, V. Breedveld and H. W. Beckham, *Macromolecules*, 2009, **42**, 3121–3128.
25 T. Vettorel, A. Y. Grosberg and K. Kremer, *Phys. Biol.*, 2009, **6**, 025013.
26 Y. B. Yang, Z. Y. Sun, C. L. Fu, L. J. An and Z. G. Wang, *J. Chem. Phys.*, 2010, **133**, 064901.
27 S. Habuchi, N. Satoh, T. Yamamoto, Y. Tezuka and M. Vacha, *Angew. Chem., Int. Ed.*, 2010, **49**, 1418–1421.
28 J. Roovers and P. M. Toporowski, *J. Polym. Sci., Part B: Polym. Phys.*, 1988, **26**, 1251–1259.
29 C. W. Bielawski, D. Benitez and R. H. Grubbs, *Science*, 2002, **297**, 2041–2044.
30 D. J. Orrah, J. A. Semlyen and S. B. Ross-Murphy, *Polymer*, 1988, **29**, 1452–1454.
31 R. M. Robertson and D. E. Smith, *Macromolecules*, 2007, **40**, 3373–3377.
32 W. W. Graessley, *Adv. Polym. Sci.*, 1982, **47**, 67–117.
33 P. J. Mills, J. W. Mayer, E. J. Kramer, G. Hadziioannou, P. Lutz, C. Strazielle, P. Rempp and A. J. Kovacs, *Macromolecules*, 1987, **20**, 513–518.
34 J. Roovers, *Macromolecules*, 1985, **18**, 1359–1361.
35 J. D. Halverson, G. S. Grest, A. Y. Grosberg and K. Kremer, *Phys. Rev. Lett.*, 2012, **108**, 038301.
36 G. B. McKenna and D. J. Plazek, *Polym. Commun.*, 1986, **27**, 304–306.
37 S. F. Tead, E. J. Kramer, G. Hadziioannou, M. Antonietti, H. Sillescu, P. Lutz and C. Strazielle, *Macromolecules*, 1992, **25**, 3942–3947.
38 T. Cosgrove, M. J. Turner, P. C. Griffiths, J. Hollingshurst, M. J. Shenton and J. A. Semlyen, *Polymer*, 1996, **37**, 1535–1540.
39 E. von Meerwall, R. Ozisik, W. L. Mattice and P. M. Pfister, *J. Chem. Phys.*, 2003, **118**, 3867–3873.
40 B. V. S. Iyer, A. K. Lele and S. Shanbhag, *Macromolecules*, 2007, **40**, 5995–6000.
41 M. Muller, J. P. Wittmer and M. E. Cates, *Phys. Rev. E: Stat. Phys., Plasmas, Fluids, Relat. Interdiscip. Top.*, 1996, **53**, 5063–5074.
42 R. M. Robertson, S. Laib and D. E. Smith, *Proc. Natl. Acad. Sci. U. S. A.*, 2006, **103**, 7310–7314.
43 S. Laib, R. M. Robertson and D. E. Smith, *Macromolecules*, 2006, **39**, 4115–4119.
44 B. Efron and R. Tibshirani, *Science*, 1991, **253**, 390–395.
45 S. Shanbhag and R. G. Larson, *Phys. Rev. Lett.*, 2005, **94**, 076001.
46 D. Magatti and F. Ferri, *Appl. Opt.*, 2001, **40**, 4011–4021.
47 J. Ramirez, S. K. Sukumaran and A. E. Likhtman, *J. Chem. Phys.*, 2007, **126**, 244904.
48 J. Watanabe, B. R. Harkness, M. Sone and H. Ichimura, *Macromolecules*, 1994, **27**, 507–512.
49 S. J. Park and R. G. Larson, *J. Rheol.*, 2006, **50**, 21–39.
50 R. Vasquez and S. Shanbhag, *Macromol. Theory Simul.*, 2011, **20**, 205–211.

 This journal is © The Royal Society of Chemistry 2012